

## Opacity effects on hydrogenlike x-ray lines emitted from laser-driven implosions

N. D. Delamater, C. F. Hooper, Jr., R. F. Joyce, and L. A. Woltz  
*University of Florida, Gainesville, Florida 32611*

N. M. Ceglio, R. L. Kauffman, and R. W. Lee  
*Lawrence Livermore National Laboratory, University of California, Livermore, California 94550*

M. C. Richardson  
*Laboratory for Laser Energetics, The University of Rochester, Rochester, New York 14623*  
 (Received 29 May 1984)

Glass microballoons filled with mixtures of argon and neon were imploded using the University of Rochester 24-beam  $\Omega$  laser system. Experimentally observed Lyman-series x-ray lines were analyzed to determine plasma core parameters and the effects of opacity on spectroscopic diagnostics. The analysis produced results which were at odds with some previous assumptions.

Stark broadening of x-ray lines has been a principal diagnostic for determining the core densities of imploded microballoons in inertial-confinement fusion research. Some previous spectroscopic studies<sup>1,2</sup> have utilized a detailed atomic physics model using hydrodynamic input data and Stark or Voigt line shapes to calculate a theoretical spectrum for comparison with experiment. This approach has produced qualitative agreement in those implosion experiments which minimize opacity effects or are well characterized in hydrodynamic simulations. Several previous spectroscopic studies<sup>3,4</sup> of laser-driven implosions have assumed that better diagnostics result when several spectral lines of given sequence are fit self-consistently for both electron density and ion density (opacity). Generally, such procedures have been only partially successful: especially for the most optically thick lines, no self-consistency has been demonstrated. Further, it has been supposed that an incorrect opacity model or an incomplete treatment of implosion dynamics were responsible for the discrepancy. Hence the assumption was made that the profile analysis of lines originating from high  $n$  states, being least affected by opacity, give the most direct measure of final core density. In this study we attempt to systematically observe the effects of opacity on the diagnostics by a self-consistent analysis of x-ray spectra obtained in pellet implosions using a method which is not tied to a collisional-radiative steady-state or local thermodynamic equilibrium (LTE) model.

In a series of experiments performed at the University of Rochester Laboratory for Laser Energetics, glass microballoons filled with various Ar-Ne mixtures were imploded using the 24-beam  $\Omega$  laser system.<sup>5</sup> Pulses of 1.06- $\mu\text{m}$  light on the order of 100 ps in duration and with an energy of approximately 600 J per pulse symmetrically irradiated the pellets. The proportion of argon in the fill was varied from 5% to 100% with the intention of systematically observing the effects of opacity on radiation transport of hydrogenic lines of  $\text{Ar}^{+17}$ . Neon was added as the other fill gas to maintain the same total pressure in the microballoons and assure that the plasma  $\bar{Z}$  remained relatively constant. For microballoons having 100- $\mu\text{m}$  di-

ameters and 1- $\mu\text{m}$  wall thicknesses, x-ray line spectra were obtained for Ar-Ne fill ratios of 25/75, 50/50, 100/0; total fill pressures were  $\sim 10$  atm.<sup>6</sup> In addition to x-ray line spectra, x-ray images of the imploded cores were obtained using x-ray microscopes and coded zone plates.

The shots analyzed provided good-quality spectral data for the Lyman-series lines of  $\text{Ar}^{+17}$  (e.g., Ly- $\alpha$ , - $\beta$ , - $\gamma$ , - $\delta$ , - $\epsilon$ ). The data was fitted using theoretical Stark- and Doppler-broadened profiles which were further broadened by the effects of opacity and an instrumental width which was assumed to have a Gaussian form with an estimated full width at half maximum of 3.5 eV. The opacity formula employed in our analysis is that appropriate for the normally emergent intensity from a uniformly emitting and absorbing slab<sup>7</sup>

$$I_\nu(l) = S_\nu(1 - e^{-\tau_\nu(l)}), \quad (1)$$

where  $S_\nu$  is the source function and the optical depth  $\tau_\nu(l)$  is given by

$$\tau_\nu(l) = (1.44 \times 10^6) \phi_\nu f_{1j} n_1 l, \quad (2)$$

where the constant is calculated for the Ar ion mass,  $\phi_\nu$  is the Stark profile in units of  $\text{eV}^{-1}$ ,  $f_{1j}$  is the oscillator strength for the Lyman series transitions,  $l$  is the slab thickness (cm), and  $n_1$  is the hydrogenic  $\text{Ar}^{+17}$  ground-state density ( $\text{g}/\text{cm}^3$ ). The slab depth  $l$  was assumed to be related to a spherical diameter  $d = \alpha l$ , where  $\alpha$  was chosen such that the intensity profiles from the slab and sphere are equivalent. Corrections from a more complete opacity model to account for a non-LTE source function in a uniform medium have been considered and generally lead to a scattering trough at line center without appreciably affecting the overall shape.<sup>4</sup>

The theoretical line profiles were then fitted to the data by a least-squares procedure to obtain a high-quality fit over the entire line profile. Although no specific provision was made to ensure that area normalization was maintained, in general, the results of our fitting procedures were in good agreement with that constraint. The fits were complicated in some cases by the overlapping of

neighboring lines (e.g., Ca or K impurities from the glass shell or lines of heliumlike  $\text{Ar}^{+16}$ ). The effects of overlapping lines were treated by adjusting relative intensities, again according to a least-squares procedure. Stark profiles for the Ly- $\alpha$  and Ly- $\beta$  lines include the fine-structure effects which are observable in the spectra of high-Z elements such as argon. The Ly- $\alpha$  line is significantly broadened and altered in shape while a slight asymmetry is introduced into the Ly- $\beta$  profile.<sup>8</sup> The inclusion of fine structure places the densities inferred from the Ly- $\alpha$  line analysis into better agreement with those deduced from consideration of other Lyman lines.

A method previously introduced was employed to determine values of electron and ion densities which are consistent for all Lyman lines observed.<sup>4</sup> Here, a fit to any experimental line using an optically thin profile yields an upper limit to the inferred electron density; theoretical profiles corresponding to lower electron densities but larger ion densities can also be employed to provide a high-quality fit; quality is defined here as in Ref. 4. Lines of best fit (LBF) can be constructed for each member of the Lyman series by fitting the observed data to a number of calculated profiles covering a range of electron density and ion density [related to opacity in Eq. (2)]. In Fig. 1, for example, the experimentally determined LBF is shown

as a curve in the  $n_e$ - $n_1$  plane for each Lyman-series line observed in several shots. If it is conjectured that all of these lines are emitted under the same plasma conditions (i.e., that they are characteristic of the same time history) then their point of intersection should identify the correct value of the average electron density  $n_e$ , and the  $\text{Ar}^{+17}$  ground-state density  $n_1$ . This procedure is inherently non-LTE as the method determines ionic densities consistent with the data, and level populations are not assumed to have reached LTE values.

Image analysis of x-ray microscope and coded-zone plate data determined the approximate diameters of the imploded cores to be 40–45  $\mu\text{m}$ .<sup>9</sup> These core sizes were then included in the expression for opacity to calculate the density of  $\text{Ar}^{+17}$  ions in the ground state. Electron temperatures of approximately 1 keV were deduced from the ratio of the Ly- $\alpha$  satellite to resonance line.<sup>10</sup>

The lines of best fit for one shot, which employed a 150  $\mu\text{m} \times 2 \mu\text{m}$ , 50/50 Ar-Ne target, are shown in Fig 1(a). It is observed that a density inference of  $n_e \approx 1.5 \times 10^{23}/\text{cm}^3$  can be made on the basis of a consistent best-fit analysis for the Ly- $\alpha$ ,  $\beta$ ,  $\gamma$ , and  $\delta$  lines; similarly a consistent density of  $\text{Ar}^{+17}$  ions in the ground state was found to be  $\sim 3 \times 10^{21}/\text{cm}^3$ . It is estimated that a 20% uncertainty in the theoretical line profiles results in a corresponding un-

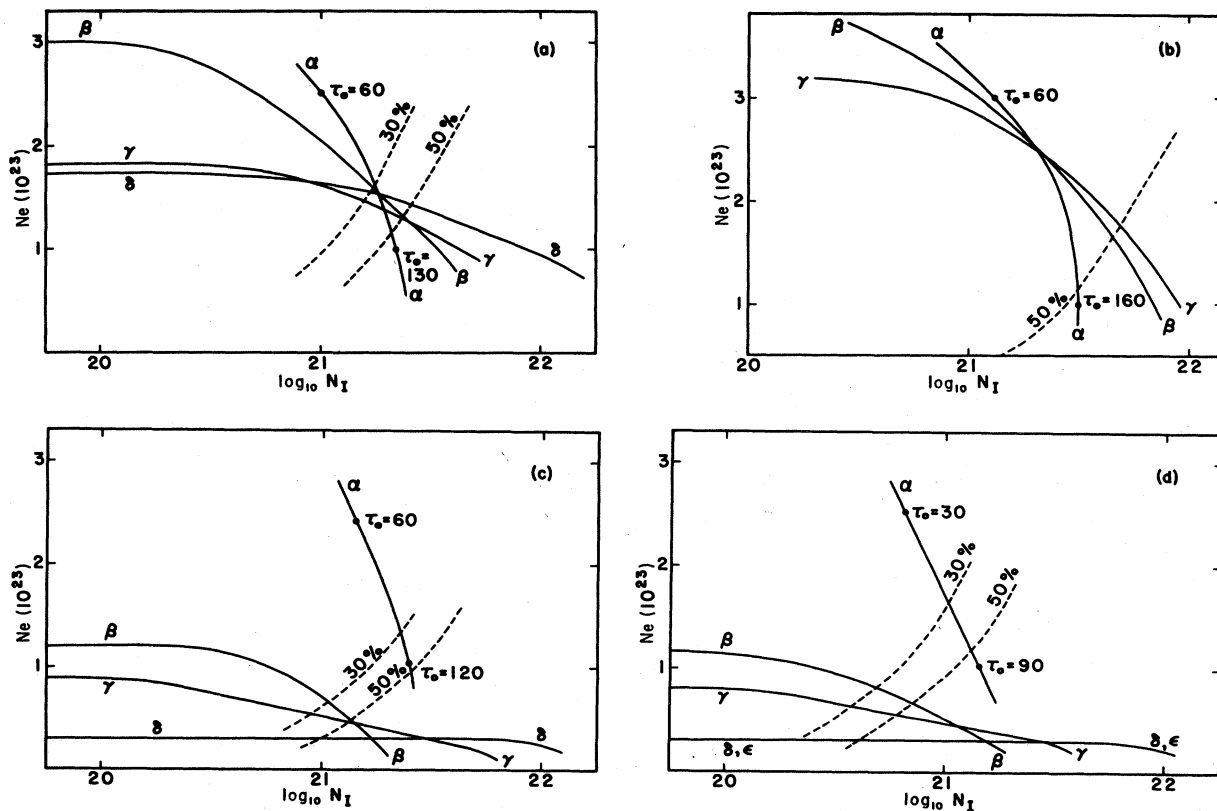


FIG. 1. Lines of best fit (LBF) for the Lyman-series members plotted in the  $n_e$ - $n_1$  plane. The electron density  $n_e$  is in number per cc,  $n_1$  in the density of ions in the  $\text{Ar}^{+17}$  ground state. The value of  $n_e$  inferred from optically thin profiles is represented by the intersection of the LBF with the ordinate. At lower densities opacity broadening must be included (added) to assure a good fit. Dashed limit lines refer to constraints imposed on  $n_1$  through the use of ionization equilibrium models.  $\tau_0$  signifies the calculated opacity at the Ly- $\alpha$  line center which is characteristic of the indicated point on the LBF.

certainty in the LBF. Errors in emission region size will directly affect the ion density determination but the electron density and the general trends indicated are not sensitive to this dimension. It was assumed that all Lyman-series lines were emitted from the same emission region, so all the LBF's would be affected equally by errors in size.

The ionization-limit curves shown in Fig. 1(a) correspond to 30% and 50% of the total argon ions in the ground state of  $\text{Ar}^{+17}$ . An upper bound on the  $\text{Ar}^{+17}$  ionic ground-state density appears to be 50%, regardless of the ionization model.<sup>4,11</sup> Hence the 50% line defined in the  $n_e$ - $n_1$  plane represents a limit: all physically realizable results are excluded from the region to the right of that curve. The LBF analysis of the shot in Fig. 1(a) implies an  $\text{Ar}^{+17}$  ground-state density which includes roughly 30–50% of the total argon ions.

The lines of best fit for another shot, one which employed a  $100\ \mu\text{m} \times 3\ \mu\text{m}$  100% Ar filled target, are shown in Fig. 1(b). It is observed that the Ly- $\alpha$ , - $\beta$ , and - $\gamma$  LBF are consistent with  $n_e = 2.5 \times 10^{23}/\text{cm}^3$  and  $n_1 = 2.1 \times 10^{21}/\text{cm}^3$ . As in the previous case [Fig. 1(a)], less than 50% of the total argon ions are in the  $\text{Ar}^{+17}$  ground state.

In the implosions of these thick-shelled targets, the mean free path of hot electrons is reduced, resulting in less heating of the core and a slower more ablative implosion, generally reaching higher densities.<sup>9</sup> The hydrogenic x-ray spectra from the implosions of  $150\ \mu\text{m} \times 2\ \mu\text{m}$  and the  $100\ \mu\text{m} \times 3\ \mu\text{m}$  targets allowed a self-consistent electron

and ion density determination from the analysis of all observed Lyman-series members. In fact, this is the first time that analysis of the optically thick Ly- $\alpha$  line ( $\tau_0 = 100$ ) has been consistent with that for the other series members.<sup>4</sup> We attribute this improvement, at least in part, to the inclusion of fine-structure corrections and to an extended treatment of the line wings. In these more ablative implosions the conditions of line formation appear to be equivalent, or nearly so, for all the Lyman-series members; time integration effects of the spectral data produces no serious inconsistencies. Hence, in the "right" system an optically thick line can be used as a density diagnostic.

Next we consider two examples of experiments which employed  $100\ \mu\text{m} \times 1\ \mu\text{m}$  targets. Figures 1(c) and (d) illustrate lines of best fit for shots corresponding to Ar-Ne mixtures of 100/0 and 25/75, respectively. In these shots the highest series lines,  $\delta$  and  $\epsilon$ , are observed to correspond to average densities that are best determined to be  $\leq 3 \times 10^{22}/\text{cc}$ . This density is significantly lower than that inferred from the Ly- $\alpha$ , - $\beta$ , and - $\gamma$  lines which imply  $n_e \geq 5 \times 10^{22}/\text{cm}^3$ , while assuming consistency with the 50% ionization limit. For lower electron densities, fits for these lines would require ion ground-state densities in the forbidden region, e.g., to the right of the 50% line. In any event, the  $\delta$  and  $\epsilon$  lines are seen to be too narrow to agree with the density obtained from the  $\alpha$ ,  $\beta$ , and  $\gamma$  lines. Examples of line-shape fits for the Lyman-series lines observed from the shot of Fig 1(c) are shown in Fig. 2. This

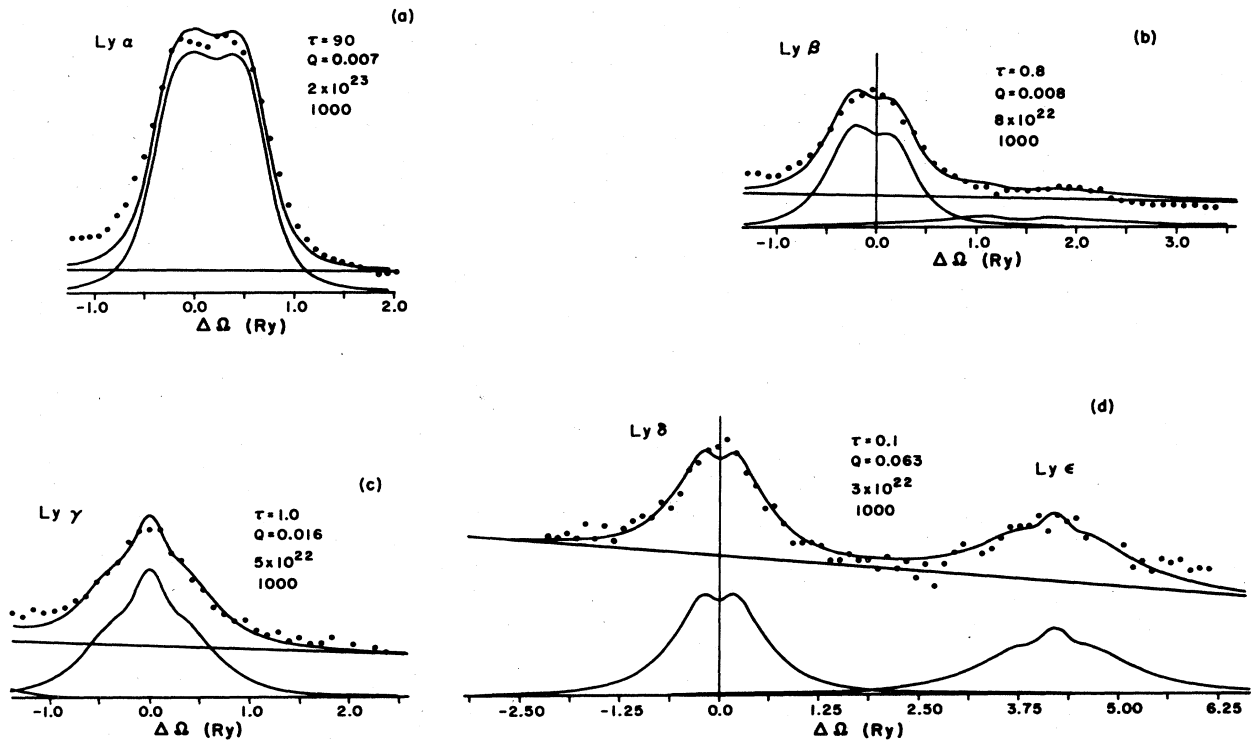


FIG. 2. Fits to the Lyman-series lines of the shot used in Fig. 1(c) are shown. Values for optical depth at line center, quality of fit, and electron temperatures and density are indicated. Experimental points are indicated by dots; solid lines indicate the intrinsic Stark and opacity broadened line shape of each component line, the continuum background fit, and the composite fit to the data.

figure illustrates both the quality of the fits obtained in this analysis, and the discrepancy in density determination from Lyman-series line-shape fits noted in the thin-shell targets.

The results of the line-fitting procedure when applied to each of the  $100\ \mu\text{m} \times 1\ \mu\text{m}$  targets did not lead to single-valued estimates of the electron and ion densities. These results suggest that different Lyman-series lines are most intense at different time intervals, and hence their profiles are representative of different temperature-density regimes. The most intense emission from the higher-lying Lyman-series members may occur earlier in time in the thin-shell targets and at higher temperatures than those occurring at peak compression; however, the emission from the lower-lying series members lasts for a longer interval and is weighted to the higher densities which occur near peak compression. The Stark-broadened profiles of the high-lying series members usually merge with the continuum at the peak densities which are attained during these implosions. High-resolution time-resolved spectroscopy is required to determine the details of these observed differences. The electron density inferred from the intersection of the Ly- $\alpha$  LBF and the 50% ionization limit line was found to be about  $1 \times 10^{23}$  per cc, regardless of fill ratio. Similarly, density inferences from the other Lyman lines showed no sensitivity to fill ratio but were also inconsistent with the Ly- $\alpha$  result. This suggests that opacity may not be as important in the diagnosis of these shots as are the effect of implosion dynamics. The implosions of these thin-shell targets can be characterized as "exploding pushers"<sup>3</sup> in contrast to those thick-shell targets used in these experiments which have a more ablative character.

Our analysis has shown that spectroscopic plasma diagnostics using Stark and opacity broadening of the Lyman-series lines from the compressed gas fill produces consistent results in the thick-shell ( $\geq 2\ \mu\text{m}$  thickness) targets, and inconsistencies in the thin-shell targets. It is sug-

gested that these inconsistencies are due both to the effects of implosion dynamics and time-integrated spectroscopy with the result that the lines from high-lying  $n$  states imply significantly lower densities than do those from the lower  $n$  states. The time-integrated spectra are consistent with a conjecture that during these implosion the line emission occurs in several bursts, corresponding to different temperature-density regimes. Thus, although it had been conjectured that lines from the highest observable series members, being the most optically thin, would provide the most accurate determination of core density, this study has been shown that lines from the lower-lying  $n$  states (e.g., Ly- $\alpha$ ,  $-\beta$ ,  $-\gamma$ ) are probably more correct in determining final core densities.

Our analysis of shots with similar target size but varying fill ratio showed similar spectral characteristics. While it was shown that opacity effects must be included for all lines, the variation of fill ratio over the range of fill pressures considered did not produce significant effects on the validity of the overall diagnostics. Future high-resolution time-resolved spectroscopy should provide further insights into the implosion dynamics.

#### ACKNOWLEDGMENTS

We would like to thank the Laboratory for Laser Energetics target fabrication group for production of the targets used in this study. The x-ray line spectra were densitometered and digitized at the Lawrence Livermore National Laboratory. Also, the authors wish to acknowledge several useful discussions with S. Skupsky and B. Yaakobi. This work was performed in part under the auspices of the U. S. Department of Energy by Lawrence Livermore National Laboratory under Contract numbers 83DP40177 and 81DP40159 and by the Laboratory for Laser Energetics under the support of the U. S. Department of Energy contract DE-AC08-80DP40124 and the sponsors of the Laser Fusion Feasibility Project.

<sup>1</sup>J. P. Apruzese *et al.*, Phys. Rev. A **24**, 1001 (1981).

<sup>2</sup>A. Hauer *et al.*, Phys. Rev. A **28**, 963 (1983).

<sup>3</sup>B. Yaakobi *et al.*, Phys. Rev. A **19**, 1247 (1979); Opt Commun. **43**, 343 (1982).

<sup>4</sup>J. D. Kilkenny, R. W. Lee, M. H. Key, and J. G. Lunney, Phys. Rev. A **22**, 2746 (1980). Our quality of fit is equivalent to the  $Q$  defined in this reference.

<sup>5</sup>J. Bunkenburg *et al.*, J. Quantum Electron. **12**, 1620 (1981).

<sup>6</sup>B. A. Brinker and J. R. Miller, J. Vac. Sci. Technol. **20**, 1079

(1982).

<sup>7</sup>D. Mihalas, *Stellar Atmospheres* (Freeman, San Francisco, 1978).

<sup>8</sup>L. A. Woltz and C. F. Hooper, Jr. (unpublished).

<sup>9</sup>N. M. Ceglio and G. F. Stone, J. Vac. Sci. Technol. **19**, 886 (1981).

<sup>10</sup>J. F. Seely, Phys. Rev. Lett. **42**, 1606 (1979).

<sup>11</sup>J. M. Shull and M. van Steenberg, Astrophys. J. Suppl. **48**, 94 (1982).